Very long life fatigue behaviors of 16Mn steel and welded joint

Yongjie Liu, Chao He, Chongxiang Huang, Muhammad K. Khan
and Qingyuan Wang[*]

*Key Laboratory of Energy Engineering Safety and Disaster Mechanics, Ministry of Education,
College of Architecture & Environment, Sichuan University, Chengdu, 610065, China*

Abstract.　Very long life fatigue tests were carried out on 16Mn steel base metal and its welded joint by using the ultrasonic fatigue testing technique. Specimen shapes (round and plate) were considered for both the base metal and welded joint. The results show that the specimens present different S-N curve characteristics in the region of 10^5-10^9 cycles. The round specimens showed continuously decreasing tendency while plate specimens showed a steep decreasing step and an asymptotic horizontal one. The fatigue strength of round specimen was found higher than plate specimen. The fatigue strength of as-welded joint was 45.0% of the base material for butt joint and 40% for cruciform as-welded joint. It was found that fracture can still occur in butt joint beyond 5×10^6 cycles. The cruciform joint has a fatigue limit in the very long life fatigue regime (10^7-10^9 cycles). Fatigue strength of butt as-welded joint was much higher as compared to cruciform as-welded joint. Improvement in fatigue strength of welded joint was found due to UPT. The observation of fracture surface showed crack mainly initiated from welded toe at fusion areas or geometric discontinuity sites at the surface in butt joint and from welded toe in cruciform joint.

Keywords:　16 Mn; very high cycle fatigue; welded joint; S-N curve; crack initiation mechanism

1. Introduction

Welding is a very important joining technique and extensively used in many engineering structures such as bridges, marine structures, ships, aircrafts, pipelines and pressure vessels etc (Radaj *et al*. 1998, Rudolph *et al*. 2002, Teng *et al*. 2003). Unfortunately, welded joints are always considered as the weakest part of the structure and prone to failure due to fatigue. Nowadays, in-service engineering structures are expected to serve beyond their original lives. Therefore, the design of high reliability and long lifetime become an important subject.

Highway bridges are often subjected to dynamic load including cyclic and/or random fluctuations. These bridges are large scale welded structures, which require extremely high fatigue durability and strength. An important characteristic of as-welded joints is the entirely independent fatigue behaviour, in comparison with that of base material properties (Puchi-Cabrera *et al*. 2009, Wang *et al*. 2009). It is considered that the fatigue fracture of weldments may occur beyond 10^8 cycles (Marines *et al*. 2003, Zhao *et al*. 2012, Sonsino 2007). However, some standards of fatigue design (e.g., Hobbacher 1997) indicate that welded joint offers unlimited life after five million

---

*Corresponding author, Professor, E-mail: wangqy@scu.edu.cn

loading cycles. Therefore, a better understanding of fatigue behaviours of welded joint, especially very high cycle fatigue behaviors, is a major concern in designing the durability of welded engineering components and structures.

The analysis methods of fatigue on welded joint was well reviewed by Fricke (2003) previously and many studies on fatigue behaviour of welded joint were summarized recently (Puchi-Cabrera *et al*. 2009). The effects of discontinuity, geometry, stress ratio and residual stress on the fatigue behaviour of welded structures have been considered (Teng *et al*. 2004, Fan *et al*. 2012). At present, fatigue design of welded structure is primarily performed using the nominal stress or hot spot stress approach with a series of classified S-N curves (Hobbacher 1996), which have been recommended by international codes (e.g., British Standards Institution 1993, European Committee for Standardization 1992, XIII-1539-96/XV-845-96 2002) (Dong 2001). Using an approach recommended by the provisions of XIII-1539-96/XV-845-96, the fatigue strengths of the base metal and butt-weld joint were investigated and evaluated according to the data obtained by the ultrasonic fatigue testing technique. Subsequently, the fracture surfaces of welded joints during 10^5 and 10^9 cycles were studied using scanning electron microscopy (SEM).

2. Experimental technique

2.1 Material

The material used in the present study was a commercial 16Mn steel. The chemical composition and mechanical properties are presented in Table 1. Fig. 1 presents the microstructure by optical microscopy (OM) analysis. It has an elastic modulus of 201 GPa, a yielding strength of 420 MPa and a tensile strength of 570 MPa.

Table 1 The chemical composition, wt%

C	Si	Mn	S	P	Al
0.15	0.38	1.36	0.00003	0.00012	0.00040

Fig. 1 Microstructure of 16Mn

(a) Round base material

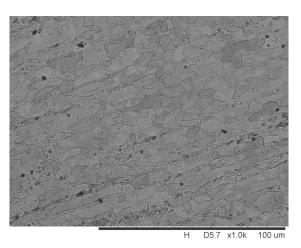(b) Plate base material

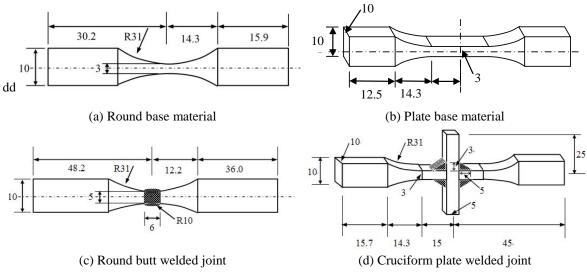(c) Round butt welded joint

(d) Cruciform plate welded joint

Fig. 2 Geometrical characteristics of specimens

2.2 Specimens

Specimens were divided into three groups: base material (round and plate), as-welded (butt and cruciform) and ultrasonic peening treatment (UPT) treated before loading. The specimens were designed to resonate longitudinally at 20 kHz, using an ultrasonic fatigue testing system as well as finite element method. The detail geometrical sizes of the specimens are shown in Fig. 2. For the cruciform plate welded joint as shown in Fig. 2(d), the horizontal plate carries the load and it is separated in two parts by the vertical plate generating four welded toes at the four corners.

2.3 Weld and treatment methods

The as-welded joints were prepared by the tungsten inert gas (TIG) arc welding method. For UPT specimen, the treatment was carried out by an air-blast machine with an outflow of 3 kg/min, a speed of 300 mm/min, a distance of 200 mm and a rotation speed of 30 *rpm*.

2.4 Fatigue test

Fatigue tests in push-pull mode were performed on a piezoelectric fatigue machine (USF-2000, made in JAPAN at 20 kHz). The experimental details were available elsewhere (Bathias 2006). The ultrasonic fatigue technique provides one practical means of generating ultra-high cycle fatigue data (Wang *et al*. 2002, 2004). A 100 to 1000 times reduction in testing time is obtained with ultrasonic fatigue when a million cycles are obtained within a minute. The tests were conducted under completely reversed cyclic loading conditions ($R=-1$) at different cyclic stresses in air and at room temperature. To reduce the increase of temperature, compressive condensing air blast and intermitted loading was adopted on specimens. Pulse loading lengths were selected with respect to the applied stress amplitudes.
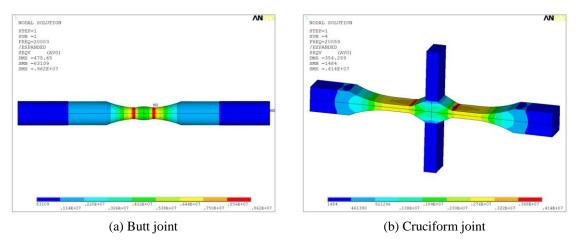
|(a) Butt joint|(b) Cruciform joint|

Fig. 3 Stress distribution in welded joints

2.5 Fractography

Fatigue fracture surfaces were investigated by scanning electron microscope (SEM) to capture the information of fatigue crack initiation and propagation mechanisms.

3. Method of processing data

3.1 Finite element analysis used for hot spot stress

Finite element program (ANSYS 13.0) was used to analyze welded joints. Owing to symmetry, only a quarter of the specimen was taken into consideration. The finite elmenent models were devleped according to geometrical characteristics of welded joints as shown in Fig. 2(c) and (d). The models consist of 7608 brick elements for butt joint and 6375 brick elements for cruciform joint, respectively. The minimum element size were 0.05mm and 0.06mm at the welded toes respecitvely in butt joint and cruciform joint. The stress distribution in the welded joints is shown in Fig. 3 (whole specimen models are given in this figure).

Hot spot stress concentration coefficient K_s could be calculated according to the correlative definition as follow

$$K_s = \sigma_{hs} / \sigma_{nom} \tag{1}$$

In this study, the coefficient K_s was calculated by the finite element analysis of welded joints and σ_{nom} represents the nominal stress in the relevant section of a smooth specimen without welded toe. Thus, the hot spot stress σ_{hs} at the fracture size could be obtained according to Eq. (1).

3.2 Calculation of the nominal stress on welded joints

According to the relation that specimens and testing system have the same vibration frequency and boundary condition, the function of vibration displacement along the axial direction of the
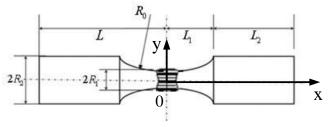
Fig. 4 Specimen

specimen (seeing Fig. 4) could be expressed as follows

$$U(x) = \begin{cases} A_0 \cos[k(L-x)], L_1 < |x| < L \\ A_0 \varphi(L_1, L_2) \dfrac{\sinh(\beta x)}{\cosh(\alpha x)}, |x| < L_1 \end{cases} \tag{2}$$

where $\quad \varphi(L_1, L_2) = \dfrac{\cos(kL_2)\cosh(\alpha L_1)}{\sinh(\beta L_1)}$, $\quad \alpha = \dfrac{1}{L_1} a\cosh\left(\dfrac{R_2}{R_1}\right)$, $\quad k = \dfrac{\omega}{c}$, $\quad c = \sqrt{\dfrac{E_d}{\rho}}$, $\quad \omega = 2\pi f$ and

$\beta = \sqrt{\alpha^2 - k^2}$. U_0 is the displacement at any end of the specimen; E_d is the dynamic Young's modulus; ρ is the density; ω is the angular frequency; f is the frequency and L_1, L_2, L, R_1, R_2 are geometrical characteristics of the specimen defined as shown in Fig. 4.

Assuming that the mechanical deformation of material obeys the Hooke's Law, the distribution function of stress (or strain) at the variable sectional region ($|x|<L_1$) could be obtained by deriving the displacement function as

$$\varepsilon(x) = A_0 \varphi(L_1, L_2) \dfrac{[\beta\cosh(\beta x)\cosh(\alpha x) - \alpha\sinh(\beta x)\sinh(\alpha x)]}{\cosh^2(\alpha x)} \tag{3}$$

$$\sigma(x) = E_d \varepsilon(x) \tag{4}$$

Therefore, the nominal stress in the fracture section could be determined by substituting the relative axial coordinate value (x) into Eq. (3) and Eq. (4).

3.3 Statistical method for the fatigue testing data

The testing data was processed according to the statistical method recommended by XIII-1539-96/XV-845-96. In this method, the fatigue lives fit the pattern of logarithmic normal distribution. Two nominal S-N curves which have the same slope m and correspond to K times of positive and negative standard deviations respectively are used to form a data distribution zone. The characteristic value (subscript K) is the nominal value of 95% survival probability associated with a two-sided 75% confidence level. The characteristic values (K index) are determined by the following procedure:

(i) Calculating log10 of all data: Stress range $\Delta\sigma$ and number of cycles N, or stress intensity factor range ΔK and crack propagation rate da/dN.

(ii) Calculating exponents m and constant $logC$ according to:

Table 2 Values of *K* for the calculation of characteristic values

n	10	15	20	25	30	40	50	100
K	2.7	2.4	2.3	2.2	2.15	2.05	2.0	1.9

$$\log N = \log C - m \log \Delta\sigma \tag{5}$$

where *C* and *m* are material coefficients.

(iii) Calculating mean C_m and standard deviation *stdv* of *logC*

$$C_m = \frac{\sum\limits_{i=1}^{n} C_i}{n} \tag{6}$$

$$stdv = \sqrt{\frac{\sum\limits_{i=1}^{n}(C_m - C_i)^2}{n-1}} \tag{7}$$

(iv) Calculating the characteristic values C_k by

$$C_k = C_m - K \cdot std \tag{8}$$

The values of *K* are given in Table 2.

4. Results and discussion

4.1 S-N curves

The plots of stress amplitude vs. number of cycle-to-failure (S-N curves) for base specimens with round and plate sections are shown in Fig. 5. It is seen that the two groups of specimens exhibit different S-N characteristics in the region of 10^5-10^9 cycles. The S-N curve of round specimens decreases linearly, while the S-N curve of plate specimens deceases sharply at stress level above 300 MPa and then almost saturates at 300 MPa. The fatigue strength of round specimen was about 20% higher than plate specimens over 10^6 cycles. The mean S-N curves can be fitted using Eq. (5).

The S-N curves of as-welded butt joints and cruciform joints are shown in Fig. 6. The stresses given in this figure are in terms of hot spot stresses. Comparing the S-N curves of base material and welding joints, it is obvious that fatigue performance of the as-welded joint is much weaker than the base material. At the same cyclic lifetime of 10^7 cycles, the fatigue strength of as-welded joint was only 45% and 60% of base material for the butt joint and cruciform joint, respectively. For butt joints and round specimen of base material, the S-N curves descend continuously without fatigue limits. However, the S-N curves of cruciform joints show two steps, a steep decreasing step above 125 MPa and an approximately saturated step at 125 MPa, which is similar to that of the plate specimen of base material. The fatigue strength of cruciform joint was only 70% of butt joint in the region of 10^5-10^9 cycles. The fatigue data of as-welded joints were analysed according to the
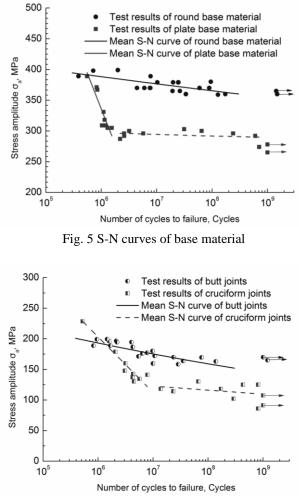
Fig. 5 S-N curves of base material

Fig. 6 S-N curves of as-welded joints

Table 3 Statistical result of fatigue test data

	m	C_m	C_k	*stdv*
But joint	15.72	42.22	41.40	0.36
Cruciform joint	7.14	21.58	20.06	0.62

statistical method (seeing 3.3) and the statistical results are shown in Table 3. Comparing the exponential coefficients of the mean S-N curves, it showed the descending rate of cruciform joint is about six times of butt joints, indicating that the fatigue life of cruciform joint is more sensitive to loading stress than butt joint possibly due to higher stress concentration at the weld toe of cruciform joint.

However, fracture can still occur on both of the two groups of as-welded joints beyond 5×10^6 cycles which showed the fatigue limit defined at lifetime of 5×10^6 cycles according the XIII-1539-96/XV-845-96 cannot guarantee a safe design.

Table 4 Comparison between the fatigue strength of base material and butt joint

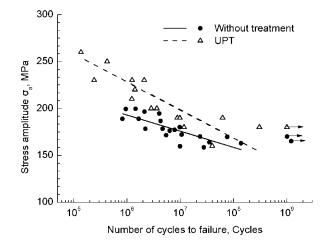| Specimen	Fatigue strength /Mpa		Dropping ratio/%
	5×10^6 cycles	1×10^9 cycles	
Base material	380	354	6.8%
Welded joint	180	145	19.4%

Fig. 7 S-N curves of joint with UPT

Table 5 Comparison between the fatigue strength of base material and butt joint

	As-welded	UPT
Fatigue strength /Mpa	180	207.4
Increase ratio / %	/	15.2

Table 4 compared the fatigue strengths between the as-welded butt joint and the base material at lifetimes of 5×10^6 and 1×10^9 cycles.

As shown in Table 4, the fatigue strengths of the welded joint and the base metal at lifetime of 1×10^9 cycles are lower than at lifetime of 5×10^6 cycles. The reduction was obvious in the welded joint where the fatigue strength at lifetime of 1×10^9 cycles was only 80.6% of lifetime of 5×10^6 cycles. The above results also show that the conditional fatigue limit of the welded joint at lifetime of 1×10^9 cycles (145 MPa) was slightly less than the value at lifetime of 5×10^6 cycles (180 MPa). The very high cycle fatigue test results showed that the fatigue limit defined at lifetime of 5×10^6 cycles cannot guarantee a safe design.

Fig. 7 shows the fatigue lives for the welded joints treated by UPT. The S-N data of the untreated welded joint were also given in this figure for comparison. It can be seen that the UPT can enhance the fatigue resistance of welded joint. In order to find out the difference between fatigue strength of specimens before and after UPT, the corresponding testing data at the cyclic number of 5×10^6 are listed and compared in Table 5. It shows the UPT for the studied conditions represents an enhancement of fatigue strength by 15.2% as compared to without treatment. Furthermore, the UPT effect on the increase of fatigue resistance was more obvious at high stress level.
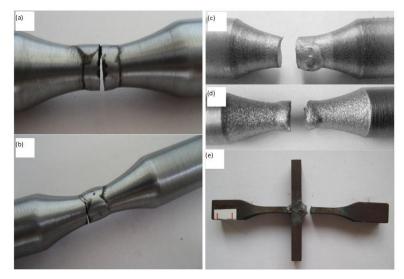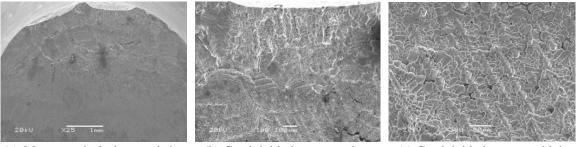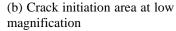
Fig. 8 Fracture site

(a) Macroscopical characteristics of fracture surface

(b) Crack initiation area at low magnification

(c) Crack initiation area at high magnification

Fig. 9 SEM micrographs of fracture surface (σ_{max}=199 MPa, N_f= 9.525×10^{5}cycles)

4.2 Fracture characteristics

4.2.1 Fracture site

The failures of fatigue specimens are shown in Fig. 8. For the butt joints, there are two typical fracture modes: (1) fatigue crack initiated at the geometric discontinuity site of welding point, as shown in Figs. 8(a) and (d); (2) fatigue failure occurred at welded toe and propagated along the bond line, as shown in Figs. 8(b) and (c). For cruciform joints, fracture surfaces were all located at welded toes, as shown in Fig. 8(e). Statistical result of failure sites showed that the fatigue behaviour of butt joints mainly occurred at the geometric discontinuity areas and welded toes, where the stress concentration is usually very high.
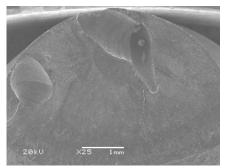
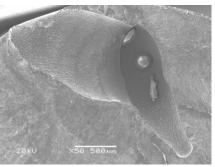### 4.2.2 Fatigue crack initiation mechanism

For as-welded butt joints, SEM observation of fracture surfaces showed fatigue crack mainly has two initiation mechanisms: fatigue failure initiated from welded defects including loose crystals and gas pores when crack initiated from geometric discontinuity site at the weld area

surface; fatigue crack initiated from internal inclusion of specimens and the discontinuity at the fusion area where crack initiated from the fusion toe.

Fig. 9 shows fracture surface of a failed specimen in the case of fatigue crack initiating from the position of geometric discontinuity at the weld area surface. Fig. 9(b) shows the microstructure of crack initiation area at high magnification. The crack initiation area has a loose characteristic structure. A distinct contour formed in welding crystallization could be clearly found. The characteristic size of the grains was measured about to 10μm shown in Fig. 9(c). The loose grain area usually becomes favourable sites for crack initiation under cyclic loading due to high stress concentration and plane stress state at the surface of the welded joint.
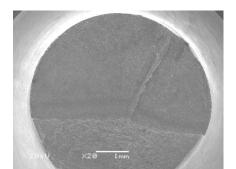
Fig. 10 shows fracture surface of a fractured specimen with fatigue crack initiation from gas pores within the welding zone.The fracture site showed weld defects of two pits formed due to the gas produced in welding did not spill-out, shown in Fig. 10(a). Fig. 10(b) shows the fractography of crack initiation areas at 50 times magnification respectively. The crack initiated from the welded gas pore and propagated outward with a tendency to the corners of the pits. No loose grain structure was observed at the crack initiation area in this case, contrasting to that shown in Fig. 9.
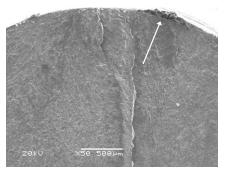
Fig. 11 shows the fracture surface of a failed specimen for crack initiating from the fusion toe. The fracture surface showed as different elevations on both sides of the main crack and the main crack grew through the propagation area, shown in Fig. 11(a). Fig. 11(b) show the fractography of crack initiation area at low and high magnification respectively. The crack initiated from a nonmetallic inclusion located beneath the specimen surface.

(a) Macroscopical characteristics of fracture surface   (b) Crack initiation area at low magnification

Fig. 10 SEM micrograph of but joint (σ_{max}=170 MPa, N_f= 7.614×10^7 cycles)

(a) Macroscopical characteristics of fracture surface   (b) Crack initiation area at low magnification

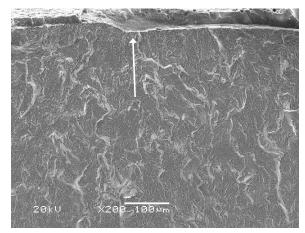Fig. 11 SEM micrograph of but joint (σ_{max}=164 MPa, N_f= 3.527×10^7 cycles)

Fig. 12 SEM micrograph of but joint (σ_{max}= 172 MPa, N_f= 1.065×10^7 cycles)
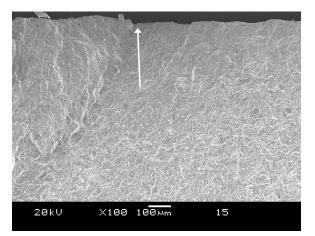

Fig. 13 SEM micrographs of cruciform joint (σ_{max}= 93 MPa, N_f= 4.300×10^8 cycles)

Moreover, the discontinuity at the fusion area always becomes favorable site for crack initiation since there has a high stress concentration, shown in Fig. 12. Thus, the fusion area of the welded joint is considered as the weak part of the specimen without welded defects, which easily causes slipping and strain concentration under cyclic stress loading.

In contrast to the butt joint, the crack initiation of cruciform joint was straight forward and it was found from SEM observations that cracks occur at the geometric discontinuity sites as shown in Fig. 13.

5. Conclusions

Ultrasonic vibration specimens of 16Mn base material and welded joint were designed and tested up to very high cycle fatigue in this study. The experimental results showed that during 10^5 and 10^9 cycles, the S-N curves of butt as-welded joints and relative round base material were continuously decreasing tendency. The S-N curves of cruciform as-welded joints and relative plate

base material specimens showed steep decreasing step and an asymptotic horizontal one. The fatigue strength of round base material specimen was higher as compared to plate base material specimen, showing a size effect. Fatigue property of welded joint was less than the base material. The fatigue strength of as-welded joint was 45% of base material for butt joint and 40% of base material for cruciform as-welded joints Fatigue strength of butt as-welded joint was higher than the cruciform as-welded joint. UPT improved the fatigue strength of welded joint by 15.2%. The observation of the fracture surface showed crack mainly initiated from welded toe at fusion area or geometric discontinuity sites at the surface in butt joint and from welded toe in cruciform joint.

Acknowledgements

References

BS7608 (1993), *Code of practice for fatigue design and assessment of steel structures*, British Standards Institution, London.
Bathias, C. (2006), "Piezoelectric fatigue testing machines and devices", *Int. J. Fatigue*, **28**, 1438-1445.
Dong, P. (2001), "A structural stress definition and numerical implementation for fatigue analysis of welded joints", *Int. J. Fatigue*, **23**, 865-876.
ENV 1993-1-1: Eurcode 3 (1992), *Design of steel structures-Part 1-1*, European Committee for Standardization, Brussels.
Fan, J.L., Guo, X.L., Wu, C.W. (2012), "Fatigue performance assessment of welded joints using the infrared thermography", *Struct. Eng. Mech*., **44**, 417-429.
Fricke, W. (2003). "Fatigue analysis of welded joints:state of development", *Mar. Struct*., **16**, 185-200.
Hobbacher, A. (1996), *Fatigue design of welded joints and components:Recommendations of IIW Joint Working Group XIII-XV*, Abington Publishing, Abington, Cambridge, UK.
Hobbacher, A. (1997), "Basic philosophy of the new IIW recommendations on fatigue design of welded joints and components", *Weld World*, **39**, 272-278.
Marines, I. and Bathias, X. (2003), "An understanding of very high cycle fatigue of matals," *Int. J. Fatigue*, **25**, 1101-1107.
Puchi-Cabrera, E.S., Saya-Gamboa, R.A., La Barbera-Sosa, J.G. *et al.* (2009), "Fatigue Llife of AISI 316L Stainless Steel Welded Joints, Obtained by GMAW", *Weld. Int*., **23**, 778-788.
Radaj, D., Sonsino, C.M. and Flade, D. (1998), "Prediction of service fatigue strength of a welded tubular joint on the basis of the notch strain approach", *Int. J. Fatigue*, **20**, 471-480.
Rudolph, J. and Weiss, E. (2002), "Concept-conforming modeling and analysis of welded pressure vessel components in the context of structural, notch stress and local strain approaches to design against fatigue", *CHEM-ING-TECH*, **74**, 33-40.
Sonsino, C.M. (2007), "Course of SN-curves especially in the high-cycle fatigue regime with regard to component design and safety", *Int. J. Fatigue*, **29**, 2246-2258.
Teng, T.L., Fung, C.P. and Chang, P.H. (2003), "Effect of Residual Stresses on the Fatigue of Butt Joints Using Thermal Elasto-plastic and Multiaxial Fatigue Theory", *Eng. Fail. Anal.*, **10**, 131-151.
Teng, T.L. and Chang, P.H. (2004), "Effect of residual stresses on fatigue crack initiation life for butt-welded joints", *J. Mater. Proc. Tech.*, **145**, 325-335.
Wang, Q.Y., Bathias, C., Kawagoishi, N. and Chen, Q. (2002), "Effect of inclusion on subsurface crack initiation and gigacycle fatigue strength", *Int. J. Fatigue*, **24**, 1269-1274.

Wang, Q.Y. and Bathias, C. (2004), "Fatigue characterization of a spheroidal graphite cast iron under ultrasonic loading", *J. Mater. Sci.*,**39**, 687-689.

Wang, T., Wang, D., Huo, L. and Zhang, Y. (2009), "Discussion on fatigue design of welded joints enhanced by ultrasonic peening treatment (UPT)", *Int. J. Fatigue*, **31**, 644-650.

XIII-1539-96/XV-845-96 (2002), *Recommendations for fatigue design of welded joints and components*, International Institute of Welding, Paris.

Zhao, X., Wang, D., Deng, C. Liu, Y. and Song, Z. (2012), "The fatigue behaviors of butt welds ground flush in the super-long life regime", *Int. J. Fatigue*, **36**, 1-8.

CC